

Supplemental Material - “Non-empirical Semi-local Free-Energy Density Functional for Matter Under Extreme Conditions”

V.V. Krasiev,^{1,2,*} James W. Dufty,³ and S.B. Trickey⁴

¹*Quantum Theory Project, Department of Physics and Department of Chemistry,
P.O. Box 118435, University of Florida, Gainesville FL 32611-8435, USA*

²*Laboratory for Laser Energetics, University of Rochester,
250 East River Road, Rochester NY 14623, USA*

³*Department of Physics, P.O. Box 118435, University of Florida, Gainesville FL 32611-8435, USA*

⁴*Quantum Theory Project, Department of Physics and Department of Chemistry,
P.O. Box 118435, University of Florida, Gainesville FL 32611-8435, USA*

I. $\tilde{B}_c(r_s, t)$ FIT

The gradient correction $g_{xc}^{(2)}(n, T)$ that is the central ingredient in Eq. (1) of the main paper was evaluated numerically in Ref. [1] with use of a relation to the static local field correction [2, 3] and quantum Monte-Carlo data for the finite-T HEG [4]. Those data together with Eq. (2) of the main paper, namely,

$$f_{xc}^{(2)}(n, \nabla n, T) = C_x^{(2)} \varepsilon_x^{\text{LDA}}(n) s^2(n, \nabla n) \tilde{B}_x(t) + C_c^{(2)} n^{1/3} s^2(n, \nabla n) \tilde{B}_c(n, t), \quad (\text{S1})$$

allow numerical evaluation of $\tilde{B}_c(r_s, t)$ ($r_s = (3/4\pi)^{1/3} n^{-1/3}$, $t = T/T_F$). The result is consistent with the assumption that the correlation gradient correction in Eq. (S1) reduces to the zero-T gradient correction when $T \rightarrow 0$, i.e., that $\lim_{T \rightarrow 0} \tilde{B}_c(r_s, t) = 1$. An analytical form for $\tilde{B}_c(r_s, t)$ then can be obtained by a technique similar to that used earlier [5]. Specifically, we fitted a Padé approximant of order [4, 5] with respect to the variable $u = t^{13/4}$ and with r_s -dependent coefficients, to wit

$$\tilde{B}_c(r_s, t) = \frac{1 + \sum_{i=1}^4 (a_i + b_i r_s^{1/2} + c_i r_s) u^i}{1 + \sum_{i=1}^5 (d_i + e_i r_s^{3/2} + f_i r_s^3) u^i}. \quad (\text{S2})$$

This form incorporates the correct zero-T limit and decreases for large T . During parametrization, $\tilde{B}_c(r_s, t)$ was checked for poles in the domain $(r_s, t) \in ([0.01, 1000], [0, 1000])$. If the denominator of Eq. (S2) had a root, that parameter set was rejected. Proper positivity also was enforced. The final set of parameters is given in Table S1. In addition to the reference data points shown in the right-hand panel of Fig. 1 of the main paper, we also used $r_s = 12$ data with the same set of t values. As to accuracy, the mean absolute relative deviation of the fit calculated over 64 reference points is 5% and the maximum relative error is 21% at $(r_s, t) = (0.5, 0.0625)$.

TABLE S1: Parameters for the $\tilde{B}_c(r_s, t)$ fit, Eq. (S2).

i	a_i	b_i	c_i
1	0.30047773E+03	-0.11166044E+03	0.32175261E+02
2	-0.38706401E+03	-0.45327975E+02	0.61853048E+02
3	0.25112237E+04	-0.14507109E+04	0.33585054E+03
4	0.52243427E+03	-0.30665095E+02	0.12874241E+03
	d_i	e_i	f_i
1	0.11077393E+03	0.12854960E+01	0.41006057E-02
2	0.32355494E+03	0.13482659E+02	0.18933118E-01
3	0.45509212E+03	0.23416018E+02	0.24295413E-04
4	0.10884352E+04	0.24480831E+02	0.18369776E-07
5	0.36112605E+00	0.32161372E-08	0.69274681E-10

The power of t used in the variable u arose from tests of the resulting GGA functional on real systems. We found that the low- t rate of increase of the fitted \tilde{B}_c had to be suppressed in comparison with the reference data to avoid negative total entropy in those calculations. Such an inconsistency of the reference data with the entropy positivity constraint might be caused by inaccuracies in the quantum Monte Carlo data at low- t or lack of finite-size corrections for the electron-electron pair-distribution function or both. At present there seems to be no way to diagnose the cause. Nor does there seem to be a general way to constrain a GGA C functional to deliver positive total entropies unfaillingly.

II. PBE CORRELATION FUNCTION H

The PBE ground-state correlation energy per particle [6] in our notation is

$$\varepsilon_c^{\text{GGA}}(n, \nabla n) = \varepsilon_c^{\text{LDA}}(n) + H(\varepsilon_c^{\text{LDA}}, \zeta = 0, q), \quad (\text{S3})$$

where $\varepsilon_c^{\text{LDA}}[n]$ is the LDA correlation energy per particle (PBE uses the Perdew-Wang parametrization [7]), ζ is the spin-polarization fraction, and q is a dimensionless density gradient (defined above Eq. (11) in the main

*Corresponding author.

Electronic address: vkarasev@lle.rochester.edu

paper). In our notation, the PBE H function is

$$H(\varepsilon_c^{\text{LDA}}, \zeta, q) = \gamma \phi^3 \times \ln \left\{ 1 + \frac{\beta_c}{\gamma} q^2 \left[\frac{1 + A_{\text{PBE}} q^2}{1 + A_{\text{PBE}} q^2 + A_{\text{PBE}}^2 q^4} \right] \right\} \quad (\text{S4})$$

$$A_{\text{PBE}} = \frac{\beta_c}{\gamma} [\exp \{-\varepsilon_c^{\text{LDA}} / (\gamma \phi^3)\} - 1]^{-1} \quad (\text{S5})$$

$$\phi(\zeta) = \frac{1}{2} [(1 + \zeta)^{2/3} + (1 - \zeta)^{2/3}] \quad (\text{S6})$$

with $\gamma = (1 - \ln 2)/\pi^2$. This H is used in Eq. (12) of the main paper with the substitutions $\varepsilon_c^{\text{LDA}}(n) \rightarrow f_c^{\text{LDA}}(n, T) \equiv f_c^{\text{corrKSDT}}(n, T)$, and $q(n, \nabla n) \rightarrow q_c(n, \nabla n, T)$.

III. CORRECTED KSDT PARAMETRIZATION

Recently it was found [8] that the original KSDT LDA XC free-energy parametrization for the HEG gives a total entropy that goes negative at large r_s values and small temperature ($r_s \gtrsim 10$ and $t \lesssim 0.1$). Almost immediately it was evident that the negative entropic contribution has negligible magnitude and the total entropy stays positive in practical calculations [9].

Ref. [10] demonstrated that the path integral Monte-Carlo data [4] used as input for the KSDT parametrization have accuracy limitations at very high temperatures ($t \geq 4$). That reference also provided accurate quantum Monte Carlo (QMC) data for the HEG potential energy at finite T , fitted those data at fixed reduced temperatures t following thermodynamic route B of Ref. [11], and found “significant deviations” between f_{xc} from those fixed- t fits and the KSDT parametrization. Ref. [10] data are for $r_s = 0.1, 0.3, 0.5, 1.0, 2.0, 4.0, 6.0, 8.0$, and 10.0 , and $t = 0.5, 1.0, 2.0, 4.0$, and 8.0 . KSDT was parametrized on earlier HEG data [4] for $r_s = 1, 2, 4, 6, 8, 10, 40$ and $t = 0.0625, 0.125, 0.25, 0.5, 1.0, 2.0, 4.0, 8.0$. The WDM density range is about $0.25 \leq r_s \leq 10$.

The deviations of KSDT from the Ref. [10] data occur for high-density, $r_s < 1$, and comparatively high-temperature, $t \geq 2$. But for those conditions, the non-interacting contribution, f_s , of the total free energy per particle $f = f_s + f_{\text{xc}}$ is dominant, $|f_{\text{xc}}| \ll |f|$. Consequently, the relative differences with respect to the total free-energy magnitude,

$$\frac{f_{\text{xc}}^{\text{Ref.9}} - f_{\text{xc}}^{\text{KSDT}}}{|f_s + f_{\text{xc}}^{\text{Ref.9}}|} \quad (\text{S7})$$

for $t = 2, 4$, and 8 always are below 0.22%. The mean absolute value of that quotient for all the available data points over the range $2 \leq t \leq 8$ and $0.1 \leq r_s \leq 10.0$ is 0.067%.

Somewhat similarly, Groth *et al.* [12] compared various HEG f_{xc} parametrizations with the QMC data. For $r_s = 1$ and $t = 8$, Ref. [12] states that KSDT “...exhibits the largest deviations of all depicted parametrizations” and that for $t = 4$ the KSDT parametrization attains

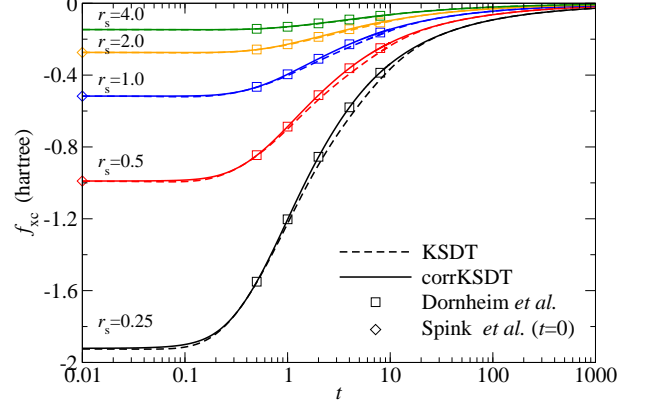


FIG. S1: Comparison between f_{xc} from the original KSDT and corrected (corrKSDT) parametrizations for the unpolarized HEG at $r_s = 0.25, 0.5, 1, 2$ and 4 . Data from Ref. [10] and the ground-state limit ($T = 0$, Ref. [13]) also are shown.

“... a maximum of $\Delta f_{\text{xc}}/f_{\text{xc}} \sim 10\%$ for $r_s = 0.1$ ”. Again, the comparison is misleading. The relative error in HEG total free-energy is 0.017% for $r_s = 1, t = 8$ and 0.0045% for $r_s = 0.1, t = 4$. Both are completely inconsequential for any DFT simulation (either LDA or GGA) of WDM.

Though these defects of the KSDT parametrization at small r_s and high t are inconsequential for DFT simulation and mostly of an aesthetic character, we scrutinized the entire KSDT fitting procedure. This uncovered a procedural mistake, namely the use of the $T=0$ K QMC data from the analytical fit provided in Ref. [13] and not the actual QMC data. Despite the differences being very small (0.15% or less), the mistake introduced the HEG negative entropy. A refit of the KSDT parameters that control the zero- T limit to the correct $T=0$ K QMC data [13] was done. Simultaneously new QMC data for the potential energy (V) for $t \geq 0.5$, from Table II of Ref. [10], were combined with accurate data for V generated from the original KSDT fit for $t = 0.0625, 0.125$, and 0.250 and $r_s = 0.1, 0.3, 0.5, 1.0, 2.0, 4.0, 6.0, 8.0$, and 10.0 . Accuracy of the original KSDT fit at low temperatures ($t \leq 0.5$) was confirmed in Refs. [14] (see Figs. 5 and S1) and [10] (see Fig. 4). HEG entropy positivity was enforced for all r_s below the first HEG phase transition, spin polarization at $r_s = 75$. (Enforcement of a constraint across a phase boundary is unjustified, since parametrization has no intrinsic validity across such a boundary.) The full refit for the spin-unpolarized case was performed using thermodynamic route B (Eq. (7)) of Ref. [11]. Table S2 provides parameters for the corrected functional, corrKSDT.

Comparison between corrected and original parametrizations at selected values of (r_s, t) shows that in most cases and especially at high temperature ($t \geq 1.0$), the differences are negligible, as expected from the argument given above. The differences at low t due to correction of the zero- T QMC data are small. Most importantly, the negative entropy for the HEG in

TABLE S2: Parameters for the corrected KSDT XC free-energy functional (corrKSDT), defined by Eqs. (9)-(14) in Ref. [11] for the unpolarized ($\zeta = 0$) case. $\lambda = (4/9\pi)^{1/3}$.

b_1	0.342554
b_2	9.141315
b_3	0.448483
b_4	18.553096
b_5	$\sqrt{3/2} \lambda^{-1} b_3 = 1.054151$
c_1	0.875130
c_2	-0.256320
c_4	0.953988
d_1	0.725917
d_2	2.237347
d_3	0.280748
d_4	4.185911
d_5	0.692183
e_1	0.255415
e_2	0.931933
e_3	0.115398
e_4	17.234117
e_5	0.451437

corrKSDT begins above $r_s = 75$, far above the range of data to which the parametrization was done and far from any state conditions for a simulation. Figure S1 compares f_{xc} from the corrKSDT and KSDT fits. The accuracy of the corrKSDT parametrization is estimated to be 0.3% for the full density and temperature ranges.

IV. corrKSDT VS. RECENT RE-PARAMETRIZATION OF REF. [15]

Recently Groth *et al.* [15] reparametrized the exchange-correlation free energy of the interacting electron gas using the KSDT functional form, constraints, and thermodynamic analysis [11]. They used some newer quantum Monte Carlo data, substantially improved finite-size corrections, and assumed the Singwi-Tosi-Land-Sjölander (STLS) approximation [16] for low- t behavior. We denote that fit as KielLDA.

Comparison of the two shows that the mean absolute relative deviation (MARD) for XC free-energy per particle (f_{xc}) calculated over the 72 (r_s, t)-data points used for the corrKSDT parametrization (see previous Section) is only 0.1%. The maximum relative deviation is 0.3%. Thus the two fits practically are identical not only for DFT applications, but also for study of the HEG itself. Note that in the HEG, small changes (of order a few percent in XC free-energy) may cause significant differences in its calculated thermodynamic properties.

The closeness arises because of the replication, in Ref. [15], of the procedure developed in Ref. [11]. In addition to the thermodynamic route B (to obtain a fitted functional f_{xc} from QMC data for potential energy alone), the KSDT analytical form was used for f_{xc} . Within it, the constraint relating coefficients b_5 and b_3 derived in

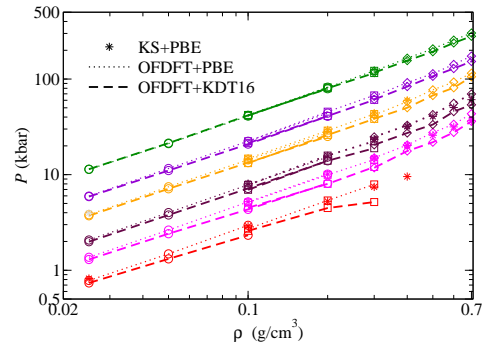


FIG. S2: Aluminum total pressure along six isotherms (10, 15, 20, 30, 40, 60 kK) for finite-T KDT16 (dashed) and ground-state PBE (dotted curves) XC functionals. Data for both functionals from AIMD simulations driven by orbital-free DFT [22–24] forces for 16 (circles), 32 (squares), or 64 (diamonds) atoms; 8500 to 16000 steps depending on T and ρ ; time-step 90-700 asec. Seemingly solid curves indicate both 16 and 32-atom data. Additional Kohn-Sham AIMD (Γ -point only) results are shown for the same numbers of atoms.

[11] to incorporate the correct high- T limit (in both spin-unpolarized and fully-polarized cases) was used and the $g_1 = 2/3$ parameter value in the spin-interpolation function was fixed from the high-density condition (see Eqs. (18)-(19) in Ref. [11] and text below). The two fits also use the same zero- T QMC data. However, KielLDA uses the STLS approximation at low- t , whereas corrKSDT avoids that extra assumption by recognizing the smallness of the error bars on original KSDT at low- t and using it for extrapolation. Both fits use almost the same set of QMC data for $t \geq 0.5$.

V. IMPLEMENTATION DETAILS

The corrKSDT LDA functional (see also [11]) provides an analytical expression for the XC free-energy per particle f_{xc}^{corrKSDT} . The corresponding correlation free-energy per particle f_c^{corrKSDT} is calculated as

$$f_c^{\text{corrKSDT}} = f_{xc}^{\text{corrKSDT}} - f_x^{\text{LDA}}, \quad (\text{S8})$$

where $f_x^{\text{LDA}} = \epsilon_x^{\text{LDA}} \tilde{A}_x(t)$ is the LDA exchange free-energy per particle, $\epsilon_x^{\text{LDA}} = -(3/4\pi)(3\pi^2 n)^{1/3}$ is the LDA ground-state exchange energy per particle, and $\tilde{A}_x(t)$ is the t -dependent factor defined by Eq. (4) in the main paper. An accurate analytical fit for $\tilde{A}_x(t)$ is given by Eq. (39) of Ref. [5] with coefficient values listed in Table 9 of that reference. For both the function $\tilde{A}_x(t)$ and its derivatives, Ref. [5] provides a detailed accuracy comparison between that representation and the Perrot-Dharma-wardana (PDW84) fit [17] which was used as an ingredient in the corrKSDT functional development. A stand-alone subroutine to evaluate $\tilde{A}_x(t)$ as well as its derivatives is available for download [18].

We note that various computational implementations of the KSDT and corrKSDT functionals are freely available [18, 19]. Implementation of the new KDT16 functional is available by request to the authors and will be made available for download shortly.

The GGA XC free-energy functional developed in this paper currently is implemented in four variants in a new version of the PROFESS@QUANTUM-ESPRESSO interface [19, 20] as well as in a locally modified ABINIT v8.4.2 package [21]. Those variants are $\nu_x = 0.21951$, $10/81$, and 0.27583 corresponding to the PBE, PBEsol, and PBEsol ground-state counterparts, plus $\nu_x = 8/81$ (see the finite-T gradient expansion Eq. (5) of the main paper). All are implemented with matching β_c values. To avoid ambiguity we denote the $\nu_x = 0.21951$, $\beta_c = 0.066725$ variant as the KDT16 func-

tional. All the calculations reported in the main paper, both Kohn-Sham and orbital-free, were performed with the PROFESS@QUANTUM-ESPRESSO package.

VI. DIRECT COMPARISON OF KDT16 AND PBE FOR LOW DENSITY AL

Fig. 4 of the main paper shows the shifts in pressures for PBE (ground state approximation) relative to KDT16 results for low-density Al along six isotherms. Fig. S2 shows the pressures themselves and illustrates how direct examination of the equation of state can conceal significant differences.

-
- [1] T. Sjöström and J. Daligault, Phys. Rev. B **90**, 155109 (2014).
 - [2] G. Niklasson, A. Sjölander, and K.S. Singwi, Phys. Rev. B **11**, 113 (1975).
 - [3] A.K. Gupta and K.S. Singwi, Phys. Rev. B **15**, 1801 (1977).
 - [4] E.W. Brown, B.K. Clark, J.L. DuBois, and D.M. Ceperley, Phys. Rev. Lett. **110**, 146405 (2013).
 - [5] V.V. Karasiev, D. Chakraborty, and S.B. Trickey, Comput. Phys. Commun. **192**, 114 (2015).
 - [6] J.P. Perdew, K. Burke, and M. Ernzerhof, Phys. Rev. Lett. **77**, 3865 (1996); erratum *ibid.* **78**, 1396 (1997).
 - [7] J.P. Perdew, and Y. Wang, Phys. Rev. B **45**, 13244 (1992).
 - [8] K. Burke, J.C. Smith, P.E. Grabowski, and A. Pribram-Jones, Phys. Rev. B **93**, 195132 (2016).
 - [9] V.V. Karasiev, L. Calderín, and S.B. Trickey, Phys. Rev. E **93**, 063207 (2016).
 - [10] T. Dornheim, S. Groth, T. Sjöström, F.D. Malone, W.M.C. Foulkes, and M. Bonitz, Phys. Rev. Lett. **117**, 156403 (2016).
 - [11] V.V. Karasiev, T. Sjöström, J. Dufty, and S.B. Trickey, Phys. Rev. Lett. **112**, 076403 (2014).
 - [12] “Free Energy of the Uniform Electron Gas: Testing Analytical Models against First Principles Results” S. Groth, T. Dornheim, and M. Bonitz, preprint, Nov. 2016.
 - [13] G.G. Spink, R.J. Needs, and N.D. Drummond, Phys. Rev. B **88**, 085121 (2013).
 - [14] T. Schoof, J. Vorberger, S. Groth, and M. Bonitz, Phys. Rev. Lett. **115**, 130402 (2015).
 - [15] S. Groth, T. Dornheim, T. Sjöström, F.D. Malone, W.M.C. Foulkes, and M. Bonitz, Phys. Rev. Lett. **119**, 135001 (2017).
 - [16] S. Tanaka, and S. Ichimaru, J. Phys. Soc. Jpn. **55**, 2278 (1986).
 - [17] F. Perrot and M.W.C. Dharma-wardana, Phys. Rev. A **30**, 2619 (1984).
 - [18] <http://www.qtp.ufl.edu/ofdft/research/computation.shtml>
 - [19] V.V. Karasiev, T. Sjöström, and S.B. Trickey, Comput. Phys. Commun. **185**, 3240 (2014).
 - [20] Paolo Giannozzi, Stefano Baroni, Nicola Bonini, Matteo Calandra, Roberto Car, Carlo Cavazzoni, Davide Ceresoli, Guido L. Chiarotti, Matteo Cococcioni, Ismaila Dabo, Andrea Dal Corso, Stefano de Gironcoli, Stefano Fabris, Guido Fratesi, Ralph Gebauer, Uwe Gerstmann, Christos Gougousis, Anton Kokalj, Michele Lazzeri, Layla Martin-Samos, Nicola Marzari, Francesco Mauri, Riccardo Mazzarello, Stefano Paolini, Alfredo Pasquarello, Lorenzo Paulatto, Carlo Sbraccia, Sandro Scandolo, Gabriele Sclauzero, Ari P. Seitsonen, Alexander Smogunov, Paolo Umari, and Renata M. Wentzcovitch, J. Phys.: Condens. Matter **21**, 395502 (2009).
 - [21] X. Gonze, F. Jollet, F. Abreu Araujo, D. Adams, B. Amadon, T. Applencourt, C. Audouze, J.-M. Beuken, J. Bieder, A. Bokhanchuk, E. Bousquet, F. Bruneval, D. Caliste, M. Côté, F. Dahm, F. Da Pieve, M. Delaveau, M. Di Gennaro, B. Dorado, C. Espejo, G. Geneste, L. Genovese, A. Gerossier, M. Giantomassi, Y. Gillet, D.R. Hamann, L. He, G. Jomard, J. Laflamme Janssen, S. Le Roux, A. Levitt, A. Lherbier, F. Liu, I. Lukačević, A. Martin, C. Martins, M.J.T. Oliveira, S. Poncé, Y. Pouillon, T. Rangel, G.-M. Rignanese, A.H. Romero, B. Rousseau, O. Rubel, A.A. Shukri, M. Stankovski, M. Torrent, M.J. Van Setten, B. Van Troeye, M.J. Verstraete, D. Waroquiers, J. Wiktor, B. Xu, A. Zhou, J.W. Zwanziger, Comput. Phys. Commun. **205**, 106 (2016).
 - [22] V.V. Karasiev, T. Sjöström, and S.B. Trickey, Phys. Rev. B **86**, 115101 (2012).
 - [23] M. Ernzerhof, J. Mol. Struct.: THEOCHEM **501-502**, 59 (2000).
 - [24] The finite-T orbital-free functional [22, 23] is very accurate for low-density Al ($\rho_{\text{Al}} \lesssim 0.8 \text{ g/cm}^3$; $T \geq 10 \text{ kK}$).